

# Orbital order in $\text{La}_{0.5}\text{Sr}_{1.5}\text{MnO}_4$ : beyond a common local Jahn-Teller picture

Hua Wu,<sup>1,2,\*</sup> C. F. Chang,<sup>1</sup> O. Schumann,<sup>1</sup> Z. Hu,<sup>1,3</sup> J. C. Cezar,<sup>4</sup> T. Burnus,<sup>1</sup>  
N. Hollmann,<sup>1</sup> N. B. Brookes,<sup>4</sup> A. Tanaka,<sup>5</sup> M. Braden,<sup>1</sup> L. H. Tjeng,<sup>1,3</sup> and D. I. Khomskii<sup>1</sup>

<sup>1</sup>*II. Physikalisches Institut, Universität zu Köln, Zùlpicher Str. 77, 50937 Köln, Germany*

<sup>2</sup>*Department of Physics, Fudan University, Shanghai 200433, China*

<sup>3</sup>*Max Planck Institute for Chemical Physics of Solids, Nöthnitzerstr. 40, 01187 Dresden, Germany*

<sup>4</sup>*European Synchrotron Radiation Facility, Boîte Postale 220, 38043 Grenoble Cédex, France*

<sup>5</sup>*Department of Quantum Matter, ADSM, Hiroshima University, Higashi-Hiroshima 739-8530, Japan*

The standard way to find the orbital occupation of Jahn-Teller (JT) ions is to use structural data, with the assumption of a one-to-one correspondence between the orbital occupation and the associated JT distortion, *e.g.* in  $\text{O}_6$  octahedron. We show, however, that this approach in principle does not work for layered systems. Specifically, using the layered manganite  $\text{La}_{0.5}\text{Sr}_{1.5}\text{MnO}_4$  as an example, we found from our x-ray absorption measurements and theoretical calculations, that the type of orbital ordering strongly contradicts the standard local distortion approach for the  $\text{Mn}^{3+}\text{O}_6$  octahedra, and that the generally ignored long-range crystal field effect and anisotropic hopping integrals are actually crucial to determine the orbital occupation. Our findings may open a pathway to control of the orbital state in multilayer systems and thus of their physical properties.

PACS numbers: 71.20.-b, 78.70.Dm, 71.27.+a, 71.70.Ch

Rich physical properties of 3d transition metal (TM) oxides are largely related to an interplay among charge, orbital, spin and lattice degrees of freedom [1, 2]. In particular, the orbital pattern plays a crucial role in magnetic exchange [3] and in many other properties. Therefore large attention is nowadays devoted to establishing the detailed type of orbital order (OO) in oxides having degenerate orbitals, and different methods can be applied. The oldest but simple and still the most widely used one is based on the assumption that there is a one-to-one correspondence between the orbital occupation and the local distortion of the nearest-neighbor anion cage around the TM ion, *i.e.* the local Jahn-Teller (JT) distortion.

For the doubly-degenerate case of  $e_g$  electrons one can characterize orbital occupation by the “mixing angle”  $\theta$ ,  $|\theta\rangle = \cos(\theta/2)|3z^2 - r^2\rangle + \sin(\theta/2)|x^2 - y^2\rangle$ . Local deformations of the oxygen octahedron around the TM ion can also be presented as a superposition of the tetragonal distortion  $Q_3$  and the orthorhombic distortion  $Q_2$ , so that the general deformation of the octahedra is  $|\theta'\rangle = \cos(\theta')|Q_3\rangle + \sin(\theta')|Q_2\rangle$ . When using the JT mechanism of electron-lattice interaction, the standard assumption, always made, is that the “mixing angles”  $\theta$  and  $\theta'$  are the same, and that the orbital mixing angle  $\theta$  is determined by the relation [3]  $\tan(\theta) = \frac{\sqrt{3}(l-s)}{2m-l-s}$ , where  $l$ ,  $m$  and  $s$  are the long, middle and short distances, respectively, from TM to the nearest-neighbor ligands, all representing a local JT distortion. This rule is usually true for isolated JT centers, and for cubic oxide materials where an additional superexchange mechanism may also get involved in determining an orbital state [1, 4]. Even in the latter case, however, after such an orbital state is established, a local distortion will in principle adjust to the orbital occupation, such that in effect again the

local distortion and the orbital occupation would be the same. But, as we will show below, this rule breaks down for certain layered systems, because not only local distortions but also the anisotropic long-range contribution to the crystal field and the electronic kinetic (band) energy play crucial role in determining the orbital state.

The half-doped single-layer manganite  $\text{La}_{0.5}\text{Sr}_{1.5}\text{MnO}_4$  turns out to be a crucial testing and battling ground for the modeling of the relationship between crystal structure, local electronic structure and the magnetic properties. On the basis of crystal structure data, resonant scattering measurements and theoretical calculations [5–10], the claim was made that the orbital pattern in the charge-ordered (CO) state of this material with the CE-type antiferromagnetic structure involves the cross-like  $x^2 - z^2 / y^2 - z^2$  type orbitals for the  $\text{Mn}^{3+}$  ions. The results seem to fit to the standard local distortion model: local structural data show that the  $\text{O}_6$  octahedra around the  $\text{Mn}^{3+}$  sites are not elongated, but rather locally compressed, with four long and two short Mn-O distances, thus ‘justifying’ the cross-like type of orbital occupation. Yet this finding is quite surprising in view of the fact that earlier various theoretical studies [11–15], not knowing the local structure around the Mn ions, proposed the rod-like  $3x^2 - r^2 / 3y^2 - r^2$  type to explain the experimentally observed magnetic structure. Also an alternative interpretation [16] of the x-ray scattering data was not considered to be persuasive.

We reinvestigated this question on high-quality single crystals of  $\text{La}_{0.5}\text{Sr}_{1.5}\text{MnO}_4$  [17–20], using polarization dependent soft x-ray absorption spectroscopy (XAS) at the Mn  $L_{2,3}$  edges [21] and multiplet cluster calculations [22–24]. We also performed density functional calculations within the local-spin-density approximation (LSDA) and LSDA plus Hubbard  $U$  (LSDA+ $U$ ) [25, 26] with a full

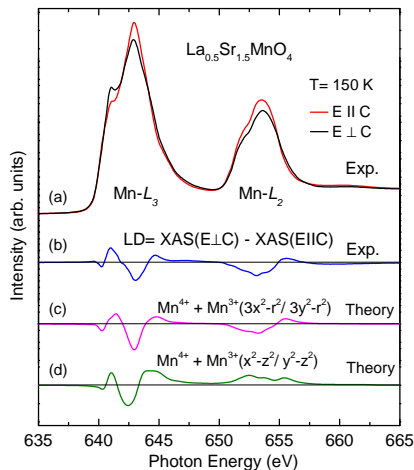


FIG. 1: (Color online) Polarization-dependent Mn- $L_{2,3}$  XAS spectra of  $\text{La}_{0.5}\text{Sr}_{1.5}\text{MnO}_4$  for  $\mathbf{E}\parallel\mathbf{c}$  (red curve) and  $\mathbf{E}\perp\mathbf{c}$  (black curve) taken at 150 K. (b) The corresponding linear dichroism (LD) spectrum. Theoretical LD calculated for orbital scenarios with (c)  $\text{Mn}^{4+} + \text{Mn}^{3+}(3x^2-r^2/3y^2-r^2)$  or (d)  $\text{Mn}^{4+} + \text{Mn}^{3+}(x^2-z^2/y^2-z^2)$  orbital occupation, each with the  $\text{Mn}^{4+} t_{2g}^3$ .

structural optimization [27], thereby staying close to the recently available structural data [9, 10]. All the experimental and computational details are given in the Supplemental Material.

Figure 1 (a) shows our polarization dependent Mn- $L_{2,3}$  XAS spectra of  $\text{La}_{0.5}\text{Sr}_{1.5}\text{MnO}_4$  for  $\mathbf{E}\parallel\mathbf{c}$  (red curve) and  $\mathbf{E}\perp\mathbf{c}$  (black curve), where  $\mathbf{E}$  is the polarization vector of the light and  $\mathbf{c}$  the crystallographic axis perpendicular to the  $\mathbf{ab}$ -plane. The spectra were taken at 150 K, i.e. below the orbital ordering temperature  $T_{\text{OO}}$  of 217 K. Curve (b) depicts the corresponding linear dichroic (LD) spectrum, defined as the difference between the two polarizations, i.e.  $\text{XAS}(\mathbf{E}\perp\mathbf{c}) - \text{XAS}(\mathbf{E}\parallel\mathbf{c})$ . We note that our spectra are very different from those reported earlier [5, 28], and we will show below that our spectra are truly representative for the  $\text{La}_{0.5}\text{Sr}_{1.5}\text{MnO}_4$  system.

To obtain some basic information concerning the orbital occupation of the  $\text{Mn}^{3+}$  ions, we can make use of a sum rule on the LD spectrum [29]. Integrating the LD spectrum throughout the  $L_{2,3}$  range, we find readily a negative net value. Since the  $\text{Mn}^{4+}$  ions have the half-filled  $t_{2g}^3$  shell configuration, their contribution to the LD integral is zero. The non-zero value of the integral is then due to the  $\text{Mn}^{3+}$  ions only. The negative value directly indicates that the  $e_g$  holes have a more out-of-plane than in-plane character, meaning that the  $e_g$  electrons have their charge density more in-plane than out-of-plane. This then favors the rod-like  $3x^2-r^2/3y^2-r^2$  type of orbital occupation and directly rules out the  $x^2-z^2/y^2-z^2$  scenario.

In order to further confirm the above experimental finding, we have simulated the Mn- $L_{2,3}$  LD spectra using

the well-proven configuration interaction cluster model which includes the full atomic multiplet theory [22–24]. Figure 1(c) shows the calculated LD spectrum for the  $\text{Mn}^{3+}$  ions having the rod-like  $3x^2-r^2/3y^2-r^2$  orbital occupation while the  $\text{Mn}^{4+}$  ions are kept in  $t_{2g}^3$  configuration. We can see that all features of the experimental LD spectrum are nicely reproduced, including the negative value for the integral. As a check we also include curve (d) which depicts the LD spectrum for the  $\text{Mn}^{3+}$  ions with the cross-like  $x^2-z^2/y^2-z^2$  orbital occupation. We notice significant discrepancies with the experimental spectrum, especially at the  $L_2$  edge where the sign of the simulated LD is opposite to that of the experimental one. Obviously, the integral value of this simulation (positive) has also the wrong sign.

We would like to remark that the excellent agreement between the simulation in curve (c) and the experimental LD spectrum can be taken as evidence that we have been able to obtain spectra which are representative for the  $\text{La}_{0.5}\text{Sr}_{1.5}\text{MnO}_4$  system. We have taken care that the high-quality single crystal was cleaved *in-situ* to obtain well ordered and clean sample area, that charging problems were avoided by using a small sample area, and that the polarization of the light rather than the sample was rotated in order to keep the same sample area to be measured for optimal comparison between the spectra taken with the two polarizations.

Thus an important aspect that emerges directly from our experimental LD and multiplet cluster calculations is that the  $\text{Mn}^{3+}$  ions have the rod-like  $3x^2-r^2/3y^2-r^2$  orbital symmetry. This is contrary to a prediction based on the local JT distortion: from the very similar in-plane 2.01 Å ( $x$ ) and the out-of-plane 1.99 Å ( $z$ ) Mn-O distances, and the shorter in-plane 1.90 Å ( $y$ ) [27], one could have expected the  $x^2-z^2$  level of  $e_g$  crystal-field to be lower. This implies a mechanism for stabilizing the rod-like  $3x^2-r^2/3y^2-r^2$  OO in this layered manganite different from the conventional local JT mechanism.

To understand better this mechanism, we have studied the electronic and magnetic structure of  $\text{La}_{0.5}\text{Sr}_{1.5}\text{MnO}_4$  and particularly the origin of  $3x^2-r^2/3y^2-r^2$  OO, using LSDA and LSDA+ $U$  calculations [25, 26] within the space group  $Bmbm$  which allows for the occurrence of the experimentally observed CO and OO. Figure 2(a) shows the orbitally resolved partial density of states (PDOS) for the two inequivalent Mn sites, calculated using LSDA+ $U$  with  $U=5$  eV and a Hund exchange energy of 0.9 eV. An insulating gap of about 1.0 eV lies between the split  $e_g$  levels. For the  $\text{Mn}^{3+}$  site, a pure  $3x^2-r^2$  level appears just below the Fermi level. The electron count is less than 1, i.e.  $0.41e$ , due to the bonding with the oxygens, as revealed by the mixed states below  $-4$  eV. For the  $\text{Mn}^{4+}$  site, the amount of occupied  $e_g$  states is only a little less than for the  $\text{Mn}^{3+}$ , but it is highly mixed  $x^2-y^2$  and  $3z^2-r^2$  hardly with any orbital polarization. Note that in spite of the  $e_g$ -electron delocalization,  $\text{La}_{0.5}\text{Sr}_{1.5}\text{MnO}_4$

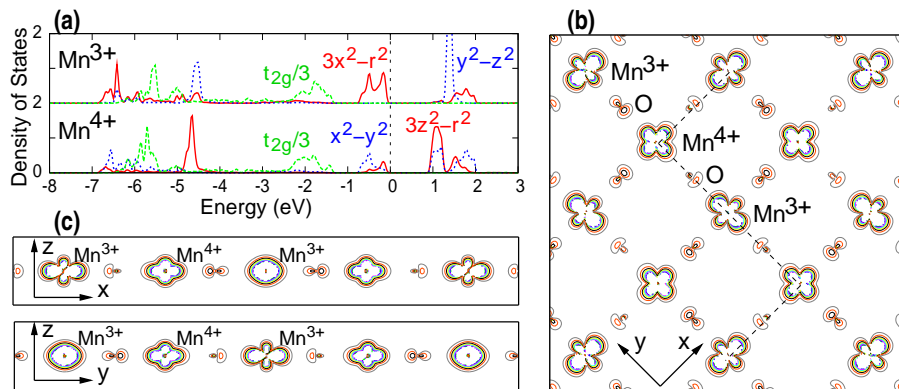


FIG. 2: (Color online) (a) PDOS of the Mn<sup>3+</sup> and Mn<sup>4+</sup> ions in the CE-type antiferromagnetic state calculated by LSDA+*U*. (b) Charge density contour plot (0.05-0.4 e/Å<sup>3</sup>) of the Mn<sup>3+</sup>-O-Mn<sup>4+</sup> network in the *xy* plane for the occupied *e<sub>g</sub>* states within 1 eV below Fermi level. The ferromagnetic zigzag chain is marked by the dashed line. (c) Charge density contour plot of the Mn<sup>3+</sup>-O-Mn<sup>4+</sup> chain in the *xz* and *yz* planes. (b) and (c) clearly show the occupied 3x<sup>2</sup>-r<sup>2</sup>/3y<sup>2</sup>-r<sup>2</sup> orbitals of the Mn<sup>3+</sup> ions.

can still be well categorized into a site-centered CO-OO system; our calculations show that this state is more stable than a bond-centered Mn-O-Mn polaronic state, by 70 meV/Mn. This site-centered CO-OO state for the half-doped case has also been confirmed by previous experimental [19] and theoretical [30] studies.

The difference between the Mn<sup>3+</sup> and Mn<sup>4+</sup> sites can also be seen in Figs. 2(b) and 2(c), where we show the *e<sub>g</sub>* charge density contour plot on the *xy* plane as well as on the *xz* and *yz* planes of the Mn-O network. One can clearly observe the 3x<sup>2</sup>-r<sup>2</sup>/3y<sup>2</sup>-r<sup>2</sup> OO at the Mn<sup>3+</sup> sites. The Mn<sup>4+</sup> ions, on the other hand, have a nearly isotropic *e<sub>g</sub>* charge density distribution. The CE-type ground state magnetic structure can be understood via the Goodenough-Kanamori-Anderson superexchange mechanisms, and this is also confirmed by our calculations: the calculations of total-energy difference between various magnetic structures allow us to derive that the ferromagnetic coupling within each zigzag chain is about -30 meV, and that the inter-zigzag-chain antiferromagnetic coupling is much weaker, being only about 2 meV. This agrees qualitatively with the inelastic neutron scattering study [19].

It is important to note that the above results remain qualitatively unchanged within a wide range of *U* values: 0-8 eV. The LSDA (*U*=0) calculation gives an insulating gap of 0.5 eV for the CE-type magnetic structure and 0.32e (0.05e) polarization for the Mn<sup>3+</sup> (Mn<sup>4+</sup>) *e<sub>g</sub>* orbitals. Switching on the *U*, the gap increases up to 1.3 eV for *U*=8 eV and the corresponding *e<sub>g</sub>* orbital polarization is 0.50e (0.05e) for the Mn<sup>3+</sup> (Mn<sup>4+</sup>). The 3x<sup>2</sup>-r<sup>2</sup>/3y<sup>2</sup>-r<sup>2</sup> type of OO is found to be *U*-independent.

As mentioned above, the obtained orbital occupation contradicts a common local JT picture. Two factors contribute to this. First, there are longer-range contributions to crystal field, cf. e.g. Refs [31, 32]. Especially in this layered manganite the coordinations of the Mn<sup>3+</sup> ion for further in-plane neighbors are very different from

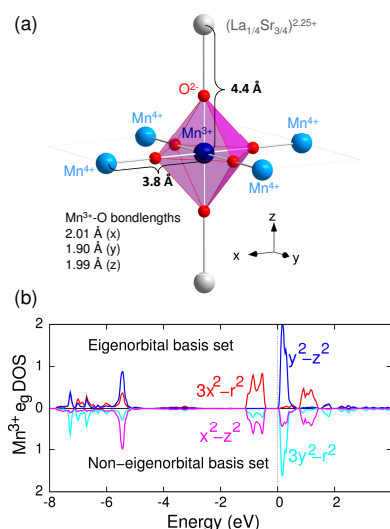


FIG. 3: (Color online) (a) A sketch of the surrounding of a Mn<sup>3+</sup> ion in La<sub>0.5</sub>Sr<sub>1.5</sub>MnO<sub>4</sub> illustrates a different contribution of the further neighbors to the crystal field. The local Mn<sup>3+</sup>-O bond lengths are also shown. (b) The Mn<sup>3+</sup> *e<sub>g</sub>* PDOS calculated by LSDA, projected onto the (3x<sup>2</sup>-r<sup>2</sup>, y<sup>2</sup>-z<sup>2</sup>) basis giving eigenstates (upper panel), and onto the (x<sup>2</sup>-z<sup>2</sup>, 3y<sup>2</sup>-r<sup>2</sup>) basis, with mixed occupation of both orbitals (lower panel).

the out-of-plane ones. The further in-plane neighbors are the Mn<sup>4+</sup> ions, which have higher valencies and are at shorter distances than the further out-of-plane neighbors, being the (Sr<sup>2+</sup>, La<sup>3+</sup>) ions, see Fig. 3(a). This has important consequences for the competition between the rod-like 3x<sup>2</sup>-r<sup>2</sup> and the cross-like x<sup>2</sup>-z<sup>2</sup> to become the lowest in energy. Our LSDA calculations reveal that the rod-like 3x<sup>2</sup>-r<sup>2</sup> orbital lies 90 meV lower than the cross-like x<sup>2</sup>-z<sup>2</sup> orbital. As a consequence, the former

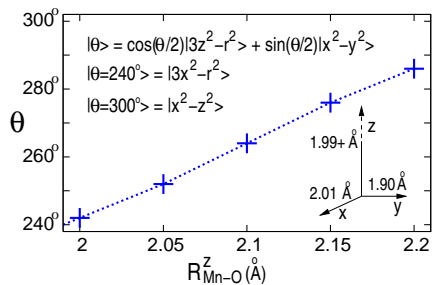


FIG. 4: (Color online) Variation of the  $\text{Mn}^{3+} e_g^1$  orbital state with respect to the  $c$ -axis Mn-O bondlength  $R^z$ , in terms of the orbital mixing angle  $\theta$  calculated by LSDA+ $U$  ( $U=5$  eV). The error bar is  $\pm 4^\circ$  for  $U = 0-8$  eV. The insets show the definition of the orbital states, and the real Mn $^{3+}$ -O bondlengths with  $R^z = 1.99$  Å at which the OO state is practically the pure  $3x^2-r^2/3y^2-r^2$  type as discussed in the main text.

becomes an occupied eigen-orbital [33], while the latter is not, i.e. the occupied  $e_g$  state of the  $\text{Mn}^{3+}$  ion is a mixture of  $x^2-z^2$  and  $3y^2-r^2$  if one chooses these orbitals as basis, see Fig. 3(b). A possible second factor is that the rod-like orbitals are more in-plane, thereby maximizing the gain in kinetic energy in this layered system. This factor is especially important for the systems close to the localized-itinerant crossover, to which our system belongs. The importance of these two factors is confirmed by recent model calculations [34].

Nevertheless, if the  $c$ -axis Mn $^{3+}$ -O bondlength were increased still further, the  $\text{Mn}^{3+} e_g^1$  state would start to deviate from the  $3x^2-r^2$  state, as seen in Fig. 4. If that bondlength exceeded 2.2 Å, the  $e_g^1$  state would become more like  $x^2-z^2$ . Note, however, that the actual stretching of the  $\text{MnO}_6$  octahedra in  $\text{La}_{0.5}\text{Sr}_{1.5}\text{MnO}_4$  along the  $c$ -direction, 1.99 Å, caused by the layered structure itself, is much less than this 2.2 Å value [27].

To summarize, using the linear dichroism and cluster model simulations of soft x-ray absorption spectroscopy, and density functional calculations, we demonstrate that  $\text{La}_{0.5}\text{Sr}_{1.5}\text{MnO}_4$  displays the rod-like  $3x^2-r^2/3y^2-r^2$  orbital ordering at Mn $^{3+}$  sites. Contrary to a common local JT picture, the observed orbital occupation strongly deviates from the one expected from the local distortion of  $\text{MnO}_6$  octahedra, i.e. the assumption that the orbital and distortion mixing angles are the same,  $\theta = \theta'$ , is violated. We explain this by considering the contribution of further neighbors to the crystal-field splitting, and by the important role of the electron kinetic energy in a system close to an insulator-metal transition. We expect that our findings are not only applicable for the ‘214’ oxides, but also for layered materials in general, including the highly topical artificial multilayer oxide systems.

This work is funded by the DFG via SFB 608.

\* Corresponding author; wu@ph2.uni-koeln.de

- [1] K. I. Kugel and D. I. Khomskii, *Sov. Phys. Usp.* **25**, 231 (1982).
- [2] Y. Tokura and N. Nagaosa, *Science* **288**, 462 (2000).
- [3] J. B. Goodenough, *Magnetism and the Chemical Bond*, (John Wiley and Sons, New York & London, 1963).
- [4] A. M. Oleś, G. Khaliullin, P. Horsch, and L. F. Feiner, *Phys. Rev. B* **72**, 214431 (2005).
- [5] D. J. Huang, W. B. Wu, G. Y. Guo, H.-J. Lin, T. Y. Hou, C. F. Chang, C. T. Chen, A. Fujimori, T. Kimura, H. B. Huang, A. Tanaka, and T. Jo, *Phys. Rev. Lett.* **92**, 087202 (2004).
- [6] S. B. Wilkins, N. Stojić, T. A. W. Beale, N. Binggeli, C. W. M. Castleton, P. Bencok, D. Prabhakaran, A. T. Boothroyd, P. D. Hatton, and M. Altarelli, *Phys. Rev. B* **71**, 245102 (2005).
- [7] N. Stojić, N. Binggeli, and M. Altarelli, *Phys. Rev. B* **72**, 104108 (2005).
- [8] K. Ebata, T. Mizokawa, and A. Fujimori, *Phys. Rev. B* **72**, 233104 (2005).
- [9] L. J. Zeng, C. Ma, H. X. Yang, R. J. Xiao, J. Q. Li, and J. Jansen, *Phys. Rev. B* **77**, 024107 (2008).
- [10] D. Okuyama, Y. Tokunaga, R. Kumai, Y. Taguchi, T. Arima, and Y. Tokura, *Phys. Rev. B* **80**, 064402 (2009).
- [11] T. Mizokawa and A. Fujimori, *Phys. Rev. B* **56**, R493 (1997).
- [12] I. V. Solovyev and K. Terakura, *Phys. Rev. Lett.* **83**, 2825 (1999).
- [13] P. Mahadevan, K. Terakura, and D. D. Sarma, *Phys. Rev. Lett.* **87**, 066404 (2001).
- [14] M. Daghofer, A. M. Oleś, D. R. Neuber, and W. von der Linden, *Phys. Rev. B* **73**, 104451 (2006).
- [15] Y. S. Lee, S. Onoda, T. Arima, Y. Tokunaga, J. P. He, Y. Kaneko, N. Nagaosa, and Y. Tokura, *Phys. Rev. Lett.* **97**, 077203 (2006).
- [16] A. Mirone, S. Dhessi, and G. van der Laan, *Eur. Phys. J. B* **53**, 23 (2006).
- [17] P. Reutler *et al.*, *J. Cryst. Growth* **249**, 222 (2003).
- [18] D. Senff *et al.*, *Phys. Rev. B* **71**, 024425 (2005).
- [19] D. Senff *et al.*, *Phys. Rev. Lett.* **96**, 257201 (2006).
- [20] D. Senff *et al.*, *Phys. Rev. B* **77**, 184413 (2008).
- [21] M. A. Hossain *et al.*, *Phys. Rev. Lett.* **101**, 016404 (2008).
- [22] F. M. F. de Groot, *J. Electron Spectrosc. Relat. Phenom.* **67**, 529 (1994).
- [23] Theo Thole Memorial Issue, *J. Electron Spectrosc. Relat. Phenom.* **86**, 1 (1997).
- [24] A. Tanaka and T. Jo, *J. Phys. Soc. Jpn.* **63**, 2788 (1994).
- [25] V. I. Anisimov *et al.*, *Phys. Rev. B* **48**, 16929 (1993).
- [26] P. Blaha, K. Schwarz, G. Madsen, D. Kvasnicka, and J. Luitz, *WIEN2k* (2001), ISBN 3-9501031-1-2.
- [27] Our LSDA+ $U$  ( $U=5$  eV) structural relaxation gave the Mn-O bondlengths of 2.009 Å ( $x$ ), 1.901 Å ( $y$ ) and 1.985 Å ( $z$ ) for Mn $^{3+}$ , and of 1.864 Å ( $x$ ), 1.936 Å ( $y$ ) and 1.980 Å ( $z$ ) for Mn $^{4+}$ . The corresponding LSDA values are 1.985, 1.884 and 1.973 Å for Mn $^{3+}$ , and 1.899, 1.943 and 1.982 Å for Mn $^{4+}$ . Both sets of data are in good agreement (within 0.02 Å) with the neutron diffraction results of O. Schumann *et al.* (to be published).
- [28] M. Merz, P. Reutler, B. Büchner, D. Arena, J. Dvorak, Y. U. Idzerda, S. Tokumitsu, and S. Schuppler, *Eur. Phys. J. B* **51**, 315 (2006).

- [29] S. I. Csiszar *et al.*, Phys. Rev. Lett. **95**, 187205 (2005).
- [30] D. V. Efremov *et al.*, Nature Mater. **3**, 853 (2004).
- [31] E. Pavarini, S. Biermann, A. Poteryaev, A. I. Lichtenstein, A. Georges, and O. K. Andersen, Phys. Rev. Lett. **92**, 176403 (2004).
- [32] Z. Fang, N. Nagaosa, and K. Terakura, Phys. Rev. B **69**, 045116 (2004).
- [33] J. van den Brink *et al.*, Phys. Rev. Lett. **83**, 5118 (1999).
- [34] A. O. Sboychakov *et al.*, [arxiv.org/abs/1007.4814](https://arxiv.org/abs/1007.4814)